Electrochemical Analysis of Tanshinone IIA in Salvia Based on Chitosan-coated Graphene

Haiyan Li * *and Shuangjiang Zan*

Department of Pharmacy, Tianjin Fourth Central Hospital, No.1, Zhongshan Road, Tianjin, Hebei District, 300140, P.R. China
*E-mail: haiyanli_luna@yeah.net

In this work, tanshinone IIA (TAN) was successfully detected using an effective and facile electrochemical sensor based on an RGO/Au (reduced graphene oxide/gold nanoparticle)-modified electrode. RGO was prepared using a microwave-assisted technique. For the preparation of the RGO/Au nanocomposite, Au nanoparticles were electrodeposited onto the surface of RGO. The electrochemical response of the sensor to TAN reduction was investigated using cyclic voltammetry (CV) and electrochemical impedance spectroscopy (EIS). The electrochemical activity of TAN is significantly enhanced when using the RGO/Au-modified GCE. Our sensor shows a desirable linear response to TAN concentration in the range of 0.01 - 10 μM. Furthermore, the sensor shows potential for use in the determination of TAN in Salvia extract samples.

1. INTRODUCTION

As one of the important lipophilic bioactive ingredients isolated from the roots of Labiatae Chinese herb Salvia miltiorrhiza Bunge (Danshen), Tanshinone IIA (TAN, Phenanthro [1,2-b]furan-10,11-dione,6,7,8,9-tetrahydro-1,6,6-trimethyl) shows diverse biological activity, including the expansion of coronary arteries and an increase in myocardial blood flow, as well as the promotion of anti-bacterial, anti-oxidation and anti-platelet properties [1-4]. However, TAN suffers from several drawbacks that affect its clinical application, such as poor solubility in water (2.8 ng/mL) [5], undesirable oral bioavailability [6], susceptibility to decomposition under light [7] and high sensitivity to temperature [8, 9]. Colloidal carriers such as polymeric micelles [10], micro-emulsions [11],

emulsions [12], liposomes [13] and nanoparticles [14] have been used to demonstrate enhancement of the solubility and stability of TAN.

Though many previous studies have proposed the detection of TAN (in plasma or pharmaceuticals) using HPLC [15], LC-MS/MS [16], HPLC-MS [17], or UFLC-MS/MS [18], the detection of TAN using an electrochemical strategy has been rarely reported. The electrochemical method has many advantages, such as the requirement of relatively low-cost instrumentation, large linear dynamic range, high repeatability, sensitivity, precision, and accuracy, which has led it to be considered as an effective analytical technique [19-22]. Electroanalytical techniques can be used to resolve many challenges in the field of pharmaceutical medicine. In recent years, more sensitive pulse techniques have been developed and have led to increased application of the electroanalytical technique for component analysis of dosage-form drugs, especially using biological specimens. Carbon-based electrochemical sensors have been extensively used because they are highly biocompatible, low in cost, high in chemical stability and show acceptable charge transfer kinetics. Conventionally, pyrolytic graphite, glassy carbon and carbon fibres have been used for the preparation of the electrodes for carbon-based sensors. In recent years, sensors have been successfully prepared using carbon nanomaterials. In general, nanomaterials with dimensional sizes ranging from 1 to 100 nm can possess a large surface-to-volume ratio and high specific surface area. Therefore, carbon nanomaterials can show more desirable interfacial adsorption features and charge transfer kinetics compared with other conventional electrode materials, leading to improved electrocatalytic activity and better sensitivity [23-25].

This study demonstrates the first report of the detection of TAN using an accurate and facile electrochemical sensor based on an RGO/Au-modified GCE. The proposed sensor can be used to provide an effective evaluation of the quality of TAN, and of its pharmaceutical preparations, circulating in the market. Moreover, the sensor was found to be highly effective in determining the quantity of TAN in Salvia samples.

2. EXPERIMENTS

2.1. Chemicals

PDDA (Poly(diallyl dimethyl ammonium chloride), Mw=100000-200000 g/mol, 20 wt.%), synthetic graphite (average particle diameter <20 μm), $HAuCl_4 \cdot 3H_2O$ and Tanshinone IIA were purchased from Sigma-Aldrich and further purified before use. All other reagents used were of analytical grade. For the synthesis of phosphate buffer solution (PBS), K_2HPO_4 (0.1 M) was mixed with KH_2PO_4 (0.1 M), followed by pH adjustment. In addition, 18.2 MΩ cm Milli-Q water was used.

2.2. Preparation of the graphene-Au nanocomposite

A modified microwave heating method was used for the synthesis of reduced graphene oxide (RGO) [26]. A mixture of aqueous GO dispersion (5 mL, 0.5 g/mL) and PDDA solution (5 mL, 1

mg/mL) was sonicated for 30 min, followed by pH adjustment to 12.0. GO was reduced and surface functionalized by heating under microwave radiation for 5 min. The as-prepared mixture was placed in a centrifuge at 10000 rpm for 10 min and then decanted yielding a black sediment (i.e., RGO). After rinsing 3 times with water, RGO was left to dry in an oven at 70°C for 12 h. For the preparation of RGO/Au/GCE, RGO and Au NPs were deposited onto a GCE. The GCE was first polished using an alumina-water slurry, and then rinsed with ethanol and water. The RGO/GCE was prepared by drop-casting an RGO dispersion (5 μL, 1 mg/mL) onto the as-prepared GCE. After thorough drying of the as-prepared RGO/GCE at 25°C, Au NPs were electrochemically deposited onto the modified GCE. Chronoamperometry was carried out in an electrolyte of 0.5 M H_2SO_4 solution containing 1% $HAuCl_4$ at -0.2 V for 1 min, using a three-electrode configuration, where the working, reference, and auxiliary electrodes were RGO/GCE, Ag/AgCl (3 M KCl), and a platinum wire, respectively.

2.3. Characterization

For XRD measurements (2θ: 5° - 80°), a Bruker D8 Advance with Cu Kα radiation ($\lambda = 0.1546$ nm) was used. Raman spectroscopy was carried out using a Raman Microprobe (Renishaw RM1000). Optical analysis was carried out using a UV-vis spectrophotometer (Perkin Elmer Lambda 950). The elemental composition of samples was characterized using a scanning electron microscope (SEM, S-4700, Hitachi High Technologies Corporation) coupled with EDX. A CHI430A electrochemical workstation with a three-electrode configuration was used for all electrochemical measurements, where the working, reference, and auxiliary electrodes were RGO/Au-modified GCE, Ag/AgCl, and a Pt wire, respectively. Samples were characterized using electrochemical impedance spectroscopy (EIS) in a multi-impedance test configuration, with an AC amplitude of 10 mV and a frequency range from 10 kHz to 10 mHz. CV was carried out at a scan rate of 100 mV/s over a potential range of -0.4 to 0.4 V. SWASV was used with a potential scan from −900 mV to 0 mV, SW amplitude of 25 mV, frequency of 100 Hz, step height of 8 mV, step time of 150 ms, pulse time of 5 ms and a current sampling time that covered the last 3 ms of the pulse.

3. RESULTS AND DISCUSSION

RGO was obtained by the reduction of GO, as confirmed by Raman spectroscopy (a method significantly sensitive to the electronic state change in carbon materials). Typically, two bands were observed in the Raman spectra of GO and the RGO/Au nanocomposite, as shown in Fig. 1A. The D band observed at 1342 cm^{-1} corresponds to the diamondoid (breathing mode of κ-point photons of A_{1g} symmetry), whereas the G band at 1568 cm^{-1} represents the graphite (first-order scattering of E_{2g} phonons by sp^2 carbon atoms). In comparison with GO, the RGO/Au nanocomposite shows a higher ratio for the intensity of the D band over the G band (I_D/I_G), indicating that the average size of the sp^2 domains is decreased and certain oxygen containing functional groups are removed in the RGO [27, 28].

Fig. 1B shows the UV-vis spectra (UVS) of GO, RGO and the RGO/Au nanocomposite. For GO, an absorption peak was observed at 227 nm, corresponding to $\pi\!-\!\pi^*$ transitions of C-C bonds. The shoulder peak observed at 314 nm results from $n\!-\!\pi^*$ transitions of C=O bonds. For RGO, only a single absorption peak was observed at 266 nm, possibly due to a redshift of the peak observed for GO. The absence of the shoulder absorption peak, and the peak redshift, shows that GO was successfully reduced into RGO. For RGO/Au, an absorption peak was observed at 545 nm, indicating surface plasmon absorption of the Au NPs. The data imply the successful electro-deposition of Au NPs onto RGO. Moreover, an absorption peak at 545 nm (due to the surface plasmon absorption of Au NPs) was observed in the spectrum recorded for the RGO/Au composite, suggesting successful electrodeposition of Au NPs onto RGO [29].
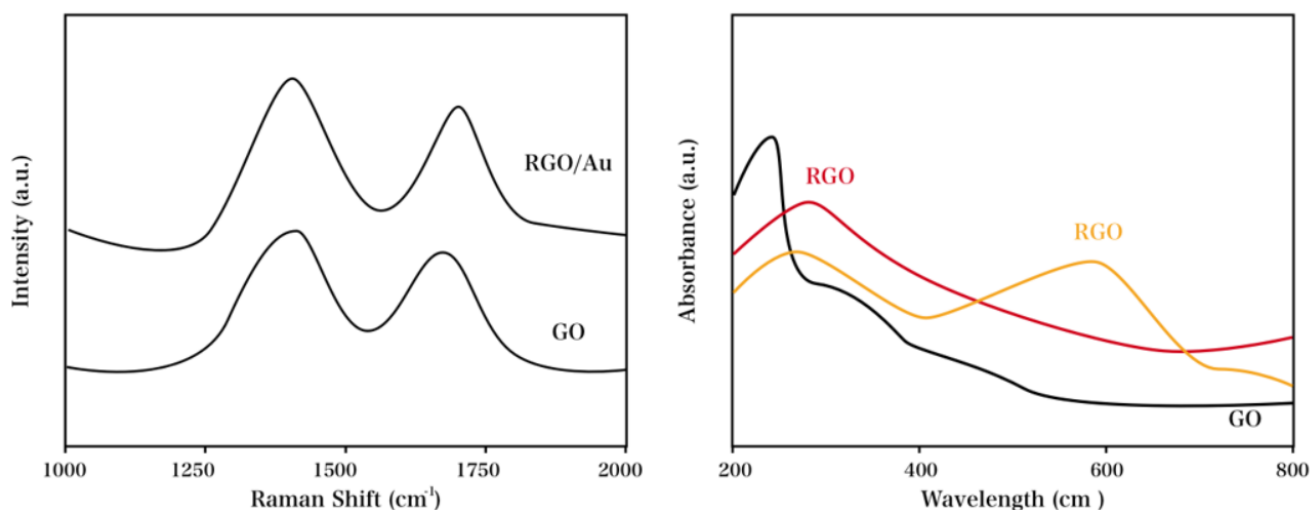

Figure 1. (A) Raman spectra of GO and RGO/Au. (B) UV-vis spectra of GO, RGO and RGO/Au nanocomposite.

RGO/Au was characterized by measurement of the EDX profiles (Fig. 2A). Elemental analysis revealed the presence of only C, O and Au, suggesting a high purity for the nanocomposite. GO, RGO and RGO/Au were also characterized via XRD profiles, as shown in Fig. 2B. GO shows a typical peak at 11.0 °, which is associated with the lattice plane (001) (*d*-spacing: 0.80 nm). The disappearance of the peak observed at 2θ of 11.0 ° in RGO suggests that GO is thoroughly reduced. Furthermore, the appearance of a broad peak (2θ: 22.8°) suggests that the RGO is composed of stacked graphene layers. For the RGO/Au nanocomposite, four diffraction peaks were observed at 38.3°, 43.6°, 63.5° and 76.9°, which correspond to the Au NP lattice planes (111), (200), (220) and (311), respectively. The weak peak at 24.08° in the RGO/Au composite confirms that exfoliated RGO is incorporated with the Au NPs [30].
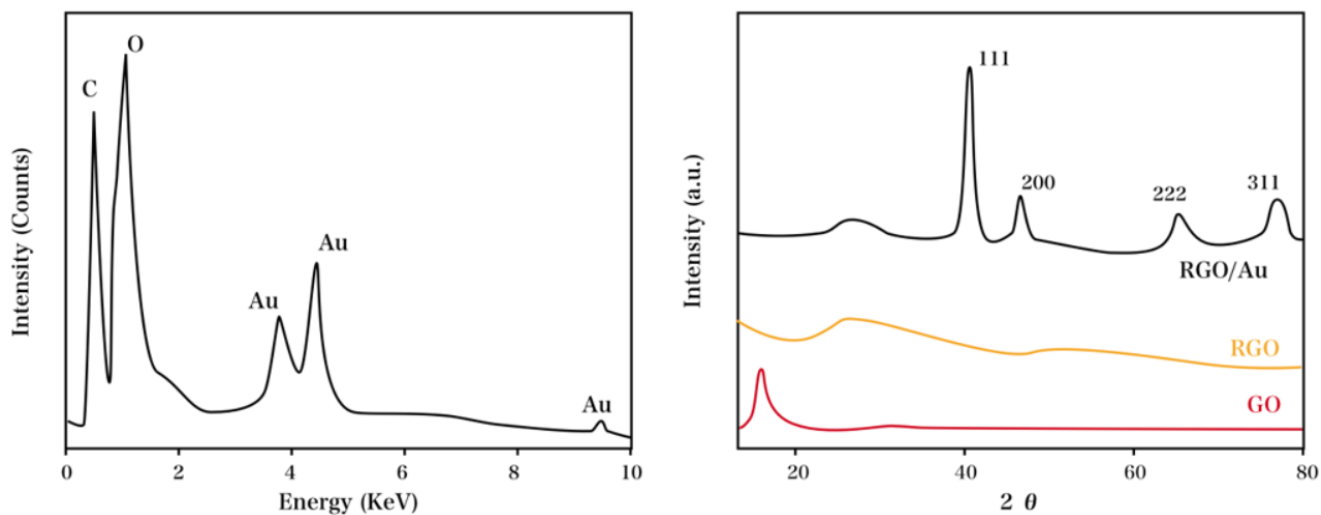
Figure 2. (A) EDX spectrum of RGO/Au composite, (B) XRD patterns of GO, RGO and RGO/Au.

The electrochemical behaviour of a GCE modified by the RGO or RGO/Au nanocomposite was investigated using electrochemical impedance spectroscopy (EIS). Typically, an EIS profile showed the superposition of a semi-circle and a straight line, suggesting the occurrence of an electron transfer process and a diffusion process, respectively. Note that the diameter of the semi-circle can be used to calculate the electron transfer resistance. Non-Faradaic impedance biosensors can be used for impedance measurement in the absence of any redox probe.
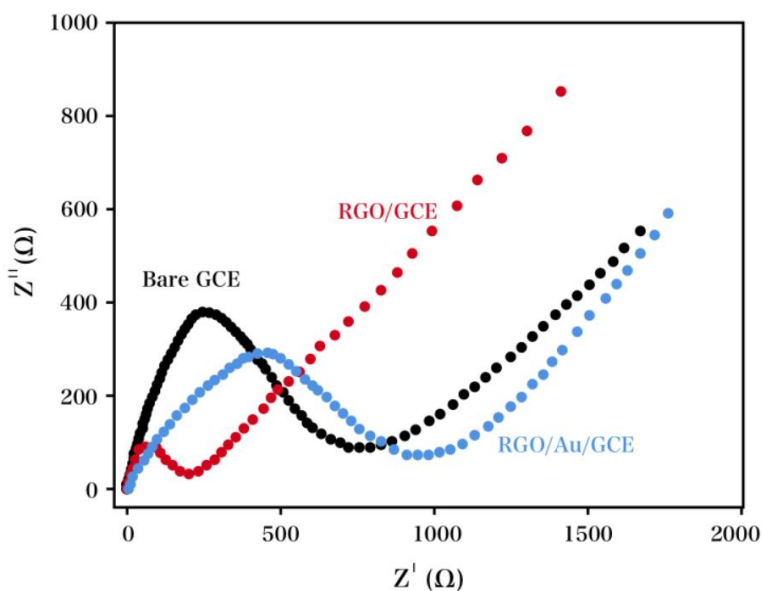

Figure 3. Nyquist diagrams obtained on bare GCE, RGO/GCE and RGO/Au/GCE electrodes.

For such sensors, bacteria detection is based on the measurement of the impedance change caused by attachment of bacterial cells to an interdigitated microelectrode in the sample solution [31]. Fig. 3 shows the performance of bare GCE, RGO-modified GCE and RGO/Au-modified GCE in $[Fe(CN)_6]^{3-/4-}$ solution (5 mM) as characterized by EIS. Compared with the bare GCE, the RGO-modified GCE showed a semi-circle with a large diameter, which suggests hindrance of electron

transfer after RGO is immobilized onto the GCE. The charge transfer in ferri/ferro cyanide can be limited by the oxygen containing groups of RGO, leading to a higher barrier for electron transfer [32]. On the other hand, the RGO/Au-modified GCE showed a smaller semi-circle diameter compared with the bare GCE, which suggests that the redox-probe has a lower electron transfer resistance. Therefore, graphene sheets can be used to modify the electrode and show enhanced electrochemical properties.

CV profiles measured for TAN (5 µM) in the presence of H_2SO_4 (0.1 M) using bare GCE (curve a), RGO-modified GCE (curve b), Au-modified GCE (curve c) and RGO/Au-modified GCE (curve d) are shown in Fig. 4. For all these electrodes, TAN shows electrochemical activation. TAN shows an exceptionally weak electrochemical response when using bare GCE, with only a few redox peaks observed. On the other hand, a significant increase in redox peak currents (ip) and an obvious decrease in ΔE_p were observed with the RGO-modified GCE or the Au-modified GCE. This suggests that the charge transfer across the electrode surface can be improved by using Au NPs and RGO, which possess desirable electrical conductivity and large surface area, thereby amplifying the electrochemical signal. Therefore, Au NPs and RGO can be used for enhancing the electrochemical properties of electrodes [33-35]. Under comparable conditions, the redox peak currents were most sensitive and well-defined for the RGO/Au-modified GCE.

TAN at varying concentrations and under optimal conditions was characterized by measurement of square wave adsorptive stripping voltammograms (SWASVs), as shown in Fig. 5. The ipa was found to depend linearly on the concentration of TAN over a range of 10 nM - 10 µM. The limit of detection was calculated to be 3 nM (S/N = 3). Therefore, the data demonstrate the detection of TAN with high sensitivity. In addition, the stability, reproducibility and repeatability of the RGO/Au-modified GCE was further investigated. To allow for comparison to previous reports, the characteristics of different electrochemical sensors for TAN are summarized in Table 1.
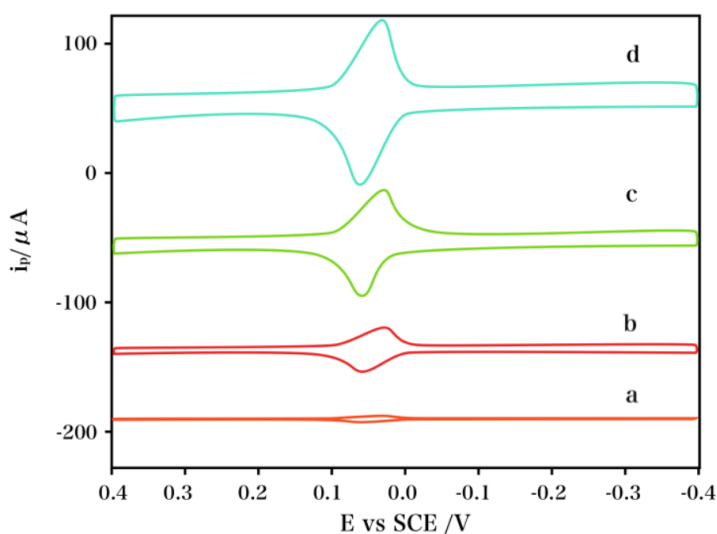

Figure 4. CV profiles of 5 µM TAN using bare GCE (curve a), RGO modified GCE (curve b), Au modified GCE (curve c), and RGO/Au/GCE (curve d) with H_2SO_4 solution (0.1 M) as the supporting electrolyte.

Table 1. Comparison of the major characteristics of electrochemical sensors used for the detection of TAN.

Electrode	Linear detection range	Detection limit	Reference
Spectroelectrochemical method	0.2 μM - 2 μM	0.03 μM	[36]
HPLC-UV	0.04 μM - 1 μM	7 nM	[37]
LC combined electrochemical detection	0.5 μM - 5 μM	0.17 μM	[38]
RGO/Au/GCE	10 nM - 10 μM	3 nM	This work

After storage for 30 days, *ca.* 92.7% of the initial current response to TAN was observed at the modified GCE, which suggests high stability for the sensor. To study reproducibility, the response of six modified electrodes towards TAN (1 μM) was investigated; the electrode response was found to show a relative standard deviation (RSD) of 5.7%. After eight successive experiments, the RSD of the response to TAN (1 μM) was determined to be 4.6%, which suggests highly repeatable detection using the sensor. These results show that determination of TAN using RGO/Au-modified GCE is highly stable, reproducible, and repeatable.
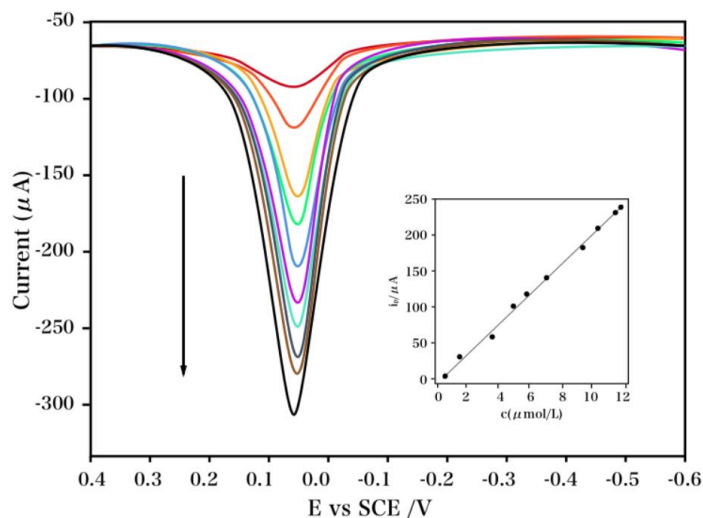
Figure 5. SWASVs and corresponding calibration plot (Inset) obtained using RGO/Au modified GCE at increased TAN concentrations under optimal conditions.

To determine the selectivity of our sensor, different interference agents were used in the presence of TAN at a constant concentration (5 μM). The tolerance limit was defined as the largest amount, yielding a relative error of < 5% for TAN detection. Fig. 6 shows that the reduction of TAN is not affected by organic compounds including uric acid, ascorbic acid, oxalic acid, glutamic acid, citric acid and glucose. Note that the data in brackets represent the molar ratio of interfering compound to TAN. It can be seen that the electrochemical sensor has a very good anti-interference property. The results discussed above indicate excellent performance for our strategy developed towards the detection of TAN.
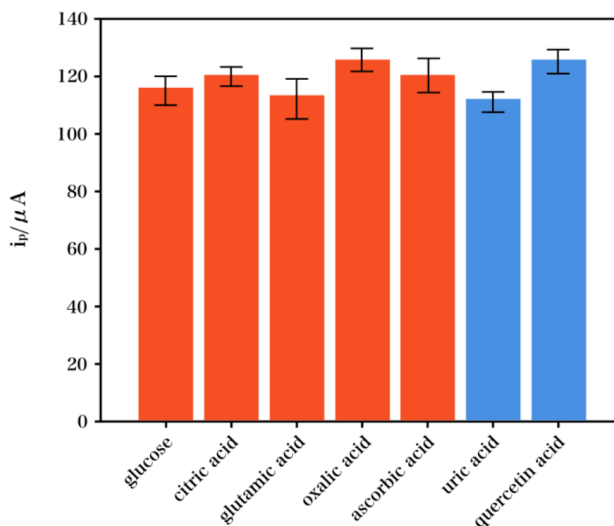
Figure 6. Interfering effects of foreign species on the voltammetric responses of TAN.

To study the practical application of our modified electrode, it was used to detect TAN in four extract samples of Salvia. Spike and recovery procedures were used in the estimation of validation, as indicated in Tab. 1. The data show that our proposed electrode exhibits desirable performance in the detection of TAN in real herb samples.

Table 1. Determination of TAN in four Salvia extract samples with RGO/Au/GCE electrode.

Sample	Addition (μM)	Found (μM)	Recovery (%)
1	0	2.41	—
	0.5	2.93	100.69
2	0	4.65	—
	1	4.59	98.71
3	0	2.53	—
	3	5.51	99.64
4	0	3.01	—
	5	8.12	101.37

4. CONCLUSIONS

In this work, a GCE was first modified with RGO using a simple chemical strategy. Electrodeposition of Au NPs onto the RGO was then used to successfully prepare an RGO/Au-modified GCE. This modified electrode was used as an electrochemical sensor for the detection of TAN. The sensor shows a linear response for a TAN concentration range of 0.01 - 10 μM. Furthermore, the sensor response was demonstrated to be highly stable and reproducible. In addition, the sensitive, reliable and facile sensor was successfully applied to the detection of TAN in extract samples of Salvia.

References

1. F. Maione, V. De Feo, E. Caiazzo, L. De Martino, C. Cicala and N. Mascolo, *Journal of ethnopharmacology*, 155 (2014) 1236.
2. C.-C. Chang, C.-F. Chu, C.-N. Wang, H.-T. Wu, K.-W. Bi, J.-H.S. Pang and S.-T. Huang, *Phytomedicine*, 21 (2014) 207.
3. X. Hao, M. Shi, L. Cui, C. Xu, Y. Zhang and G. Kai, *Biotechnology and applied biochemistry*, 62 (2015) 24.
4. S. Wang, H. Jing, H. Yang, Z. Liu, H. Guo, L. Chai and L. Hu, *Journal of ethnopharmacology*, 164 (2015) 247.
5. X. Jing, X. Wei, M. Ren, L. Wang, X. Zhang and H. Lou, *Neurochemical research*, 41 (2016) 779.
6. Q. Yu, H. Chen, L. Sheng, Y. Liang and Q. Li, *International immunopharmacology*, 22 (2014) 277.
7. M. Shi, X. Luo, G. Ju, L. Li, S. Huang, T. Zhang, H. Wang and G. Kai, *Journal of agricultural and food chemistry*, 64 (2016) 2523.
8. P. Ma, J. Liu, A. Osbourn, J. Dong and Z. Liang, *RSC Advances*, 5 (2015) 18137.
9. Y.J. Jeon, J.S. Kim, G.H. Hwang, Z. Wu, H.J. Han, S.H. Park, W. Chang, L.K. Kim, Y.-M. Lee and K.-H. Liu, *European journal of pharmacology*, 764 (2015) 480.
10. J.-P. Dai, D.-X. Zhu, J.-T. Sheng, X.-X. Chen, W.-Z. Li, G.-F. Wang, K.-S. Li and Y. Su, *Molecules*, 20 (2015) 6794.
11. Z.-L. Yu, J.-N. Wang, X.-H. Wu, H.-J. Xie, Y. Han, Y.-T. Guan, Y. Qin and J.-M. Jiang, *Journal of cardiovascular pharmacology and therapeutics*, 20 (2015) 563.
12. Y.-S. Weng, H.-F. Wang, P.-Y. Pai, G.-P. Jong, C.-H. Lai, L.-C. Chung, D.J.-Y. Hsieh, C. HsuanDay, W.-W. Kuo and C.-Y. Huang, *The American journal of Chinese medicine*, 43 (2015) 1567.
13. M.R. de Oliveira, P.F. Schuck and S.M. Dal Bosco, *Molecular neurobiology*, (2016) 1.
14. A. Zaker, C. Sykora, F. Gössnitzer, P. Abrishamchi, J. Asili, S.H. Mousavi and C. Wawrosch, *Industrial Crops and Products*, 67 (2015) 97.
15. M. Shi, X. Luo, G. Ju, X. Yu, X. Hao, Q. Huang, J. Xiao, L. Cui and G. Kai, *Functional & integrative genomics*, 14 (2014) 603.
16. L. Guo, L. Duan, X. Dong, L.-L. Dou, P. Zhou, E.-H. Liu and P. Li, *Journal of Chromatography B*, 973 (2014) 33.
17. H. He, H. Li, Y. Gao, D. Chen, L. Shi, J. Peng, S. Du and L. Chen, *Analytical Letters*, 48 (2015) 47.
18. S. Zhang, Q. Liu, H. Luo, P. Chen, X. Wu, M. Yang, W. Kong and W. Guo, *Journal of Chromatography B*, 1017 (2016) 204.
19. C. Wang, J. Du, H. Wang, C.e. Zou, F. Jiang, P. Yang and Y. Du, *Sensors and Actuators B: Chemical*, 204 (2014) 302.
20. K. Rovina and S. Siddiquee, *Food Control*, 59 (2016) 801.
21. T. Xu, N. Scafa, L.P. Xu, L. Su, C. Li, S. Zhou, Y. Liu and X. Zhang, *Electroanalysis*, 26 (2014) 449.
22. G.-X. Zhong, W.-X. Zhang, Y.-M. Sun, Y.-Q. Wei, Y. Lei, H.-P. Peng, A.-L. Liu, Y.-Z. Chen and X.-H. Lin, *Sensors and Actuators B: Chemical*, 212 (2015) 72.
23. Y. Wan, Y. Su, X. Zhu, S. Yang, J. Lu, J. Gao, C. Fan and Q. Huang, *Biosensors and Bioelectronics*, 55 (2014) 231.
24. H.-H. Li, H.-H. Wang, W.-T. Li, X.-X. Fang, X.-C. Guo, W.-H. Zhou, X. Cao, D.-X. Kou, Z.-J. Zhou and S.-X. Wu, *Sensors and Actuators B: Chemical*, 222 (2016) 1127.
25. T. Liu, X. Zhang, L. Yuan and J. Yu, *Solid State Ionics*, 283 (2015) 91.
26. W. Liu, C. Li, Y. Gu, L. Tang, Z. Zhang and M. Yang, *Electroanalysis*, (2013) 2367.
27. X. Li, Q. Wang, Y. Zhao, W. Wu, J. Chen and H. Meng, *Journal of colloid and interface science*, 411 (2013) 69.
28. S. Kamada, H. Nomoto, K. Fukuda, T. Fukawa, H. Shirai and M. Kimura, *Colloid Polym Sci*, 289

(2011) 925.

29. X.C. Lv and J. Weng, *Scientific reports*, 3 (2013)
30. C. Xu, X. Wang and J. Zhu, *J Phys Chem C*, 112 (2008) 19841.
31. S.M. Radke and E.C. Alocilja, *Biosensors & bioelectronics*, 20 (2005) 1662.
32. D.S. Jeykumari, S. Ramaprabhu and S.S. Narayanan, *Carbon*, 45 (2007) 1340.
33. J.S. Shayeh, A. Ehsani, M. Ganjali, P. Norouzi and B. Jaleh, *Applied Surface Science*, 353 (2015) 594.
34. S. Azzouzi, L. Rotariu, A.M. Benito, W.K. Maser, M.B. Ali and C. Bala, *Biosensors and Bioelectronics*, 69 (2015) 280.
35. J.S. Shayeh, A. Ehsani, A. Nikkar, P. Norouzi, M.R. Ganjali and M. Wojdyla, *New Journal of Chemistry*, 39 (2015) 9454.
36. W.-J. Li, S.-Z. Kong, H. Luo, Z.-B. Jia and Y. Cheng, *Chinese Chemical Letters*, 24 (2013) 1145.
37. Z.-r. Suo, H.-y. Qin, W. Cao, W.-z. Liu and J.-b. Zheng, *Se pu= Chinese journal of chromatography*, 23 (2005) 626.
38. J.-b. Zheng, Z.-r. Suo and L. Liu, *Chromatographia*, 63 (2006) 39